Indian Journal of Chemistry
Vol. 55A, July 2016, pp. 803-809

Notes

Solar light induced photodegradation of oxytetracyline using Zr doped TiO_2/CaO based nanocomposite

Pankaj Raizada[a,] *, Bhanu Priya[a], Pankaj Thakur[a,b] & Pardeep Singh[a]

[a]School of Chemistry, Faculty of Basic Sciences, Shoolini University, Solan (HP) 173 212, India

Email: pankajchem1@gmail.com

[b]Center for Advanced Biomaterials for Healthcare, Istituto Italiano Di Tecnologia, Naples 80125, Italy

Received 3 July 2015; re-revised and accepted 27 June 2016

Zr doped TiO_2/CaO (Zr-TiO_2/CaO) has been synthesized by sol-gel method and its photocatalytic activity tested for the removal of oxytetracycline (OTC) from aqueous solution. Zr-TiO_2/CaO has been characterized using scanning electron microscopy, transmission electron microscopy, X-ray diffraction, energy diffraction X-ray, Fourier transform infrared spectroscopy and UV-visible spectral analysis. SEM results confirm the dispersion of Zr doped TiO_2 on calcium oxide support. The Zr-TiO_2/CaO nanocomposite exhibits semicrystalline structure with average size of 50 nm. The photocatalytic activity of Zr-TiO_2/CaO has been evaluated for the photodegradation of OTC under solar light. The synergetic adsorption and photocatalysis (A+P) is most efficient for oxytetracycline removal. The effect of various reaction parameters such as OTC concentration, *p*H of reaction solution and catalyst loading has been evaluated for OTC degradation. The photocatalytic degradation of oxytetracycline obeys pseudo-first order kinetics. The nanocomposite exhibits significant recyclability due to easy separation and stability in the reaction solution. The oxidative removal occurrs through hydroxyl radical formation. The nanocomposite displays excellent photocatalytic property for degradation of oxytetracycline and may have potential applications in water treatment.

Keywords: Photocatalysis, Photodegradation, Oxytetracycline degradation, Nanocomposites, Titania, Doped titania, Zirconium doped titania, Calcium oxide

Antibiotics have been considered as emerging pollutants due to their indiscriminate use and persistence in the aquatic ecosystem[1-3]. Due to their hydrophilic property and stable naphthalene ring structure, the release of antibiotics in water bodies has been considered as a threat to aquatic environment and water bodies[4]. Moreover, the conventional methods like coagulation, flocculation, precipitation, membrane separation and aerobic biological treatment are expensive, inefficient and do not totally degrade organic pollutants[5,6]. Adsorption process generates secondary waste due to transfer of pollutants from one phase to another which further needs to be treated[5].

Photocatalysis with TiO_2 emerges as potential method for eliminating organic pollutants from water[6,7]. However, TiO_2 is an UV active photocatalyst. Recently, doping with metals and non-metals has proved to be most effective strategies to improve the photocatalytic performance of TiO_2. Many attempts have been undertaken to make TiO_2 visible light active by doping with various transition metals (e.g. Cu, Co, Ni, Cr, Mn, V, W) and non-metals (B, N, C, P, S)[8-11]. Asahi *et al.*[12] studied the effect of N doping into TiO_2 and achieved longer wavelength photo-absorption than 400 nm[12]. Cheng *et al.*[13] have reported that silica-doped TiO_2 possessed high photocatalytic activity due to the suppression of anatase to rutile phase transition and formation of oxygen vacancies[13]. Geng *et al.*[14] have stated that B atoms can be added into TiO_2 lattice either as interstitial or at the O sites with decreased the band gap.

Adsorption of pollutants onto catalyst surface is a prerequisite step for efficient photodegradation process[15-17]. However, metal oxides are poor adsorbent for aqueous phase pollutants. In this context, calcium oxide (CaO) is regarded as a potential adsorbent for waste water treatment[18]. The egg shell is regarded as better source of CaO, $CaCO_3$, $Ca(OH)_2$, calcium phosphate and hydroxyapatite in comparison to other sources such as precipitated soil, carbonaceous rock, teeth, bone and shrimp shells[19]. The hen egg shell comprises three layers, viz., outer cuticle, spongy and inner lamellar layer. The chemical composition of eggshell is calcium carbonate (94%), magnesium carbonate (1%), organic matter (4%) and calcium phosphate (1%)[20,21]. The present study focuses on the immobilization of Zr doped TiO_2 onto CaO to prepare hybrid Zr-TiO_2/CaO photocatalyst. Zr-TiO_2/CaO was characterized using scanning electron transmission (SEM), transmission electron microscopy (TEM), X-ray diffraction (XRD), energy dispersive X-ray analysis (EDX), Fourier transform infrared (FTIR) and ultraviolet-visible (UV-vis) spectroscopy. The photocatalytic efficacy of Zr-TiO_2/CaO was evaluated for the photodegradation

of oxytetracycline from aqueous phase. The effect of adsorption was tested on photocatalytic activity of Zr-TiO_2/CaO nanocomposites. The oxytetracycline removal was subjected to various reaction conditions to optimize the degradation rate. The most plausible mechanism of antibiotic degradation was also explored. The recycle efficiency of photocatalyst was tested for six consecutive cycles.

Experimental

All the chemicals used in this study were of analytical grade and used without further purification. Titanium tetraisopropoxide, isopropyl alcohol, zirconium oxynitrate, ammonia solution, oxytetracycline were obtained from SD Fine chemicals (India). The hen eggshell was collected from the local market in Solan, Himachal Pradesh (India). The hen eggshell was washed several times with distilled water and boiled for 2 h to remove any type of contamination if present. The eggshell was heated in muffle furnace at 450 °C for 2 h to obtain CaO. The obtained CaO was crushed into fine powder and preserved for further use.

Zr-TiO_2/CaO was prepared with modification in previously reported work[20]. Zr-TiO_2/CaO composite was synthesized by sol-gel method. Briefly, zirconium oxynitrate hydrate was dissolved in distilled water and resulting solution was heated at 65 °C for 30 minutes. ZrO_2 was precipitated by the gradual addition of ammonia solution (25 wt%) to the above solution till a *p*H value of 10 was reached. The obtained precipitate was then washed with ethanol and calcinated at 500 °C for 1 h. In the next step, 100 mL of 1.0 *M* titanium tetraisopropoxide solution was added to isopropyl alcohol and solution was vigorously stirred for 1 h. In another beaker, 0.1 g of ZrO_2 and 1.0 g of calcium oxide were mixed in 100 mL of distilled and solution was vigorously stirred for 30 min. Both solutions were magnetically stirred at 70 °C for 4 h. The resulting precipitate was washed with distilled water and ethanol to remove any kind of byproduct/reactants and dried at 50 °C. The obtained product was labeled as Zr-TiO_2/CaO and preserved for further use.

The photocatalytic, photolytic and adsorption experiments were performed in a double walled pyrex vessel (ht. 7.5 cm×dia. 6 cm) surrounded by thermostatic water circulation arrangement (30±0.3 °C). During equilibration experiments, slurry composed of OTC and catalyst suspension was continuously stirred. The suspension composed of OTC and Zr-TiO_2/CaO was kept under solar light with continuous stirring. At specific time intervals, aliquots (3 mL) were withdrawn and centrifuged for 2 min to remove catalyst particles from aliquot. The OTC absorbance in supernatant liquid was measured at 260 nm. The solar light intensity was measured by digital lux-meter ($35\times10^3\pm1000$ lx). Photocatalytic experiments were conducted between March to May 2014 (11 am to 2 pm). All the experiments were carried out in triplicate with errors below 5% and average values are reported. The removal efficiency was calculated using the equation, %removal of efficiency = $(C_0-C_t)/C_0$, where C_0 is the initial concentration and C_t is instant concentration of sample.

The kinetics of OTC degradation was described by pseudo-first order kinetics. The rate constant (k) and half-life period ($t_{1/2}$) were calculated from the slope of the plot of ln(c) versus t.

The *p*H of zero point charge was determined by previously reported method[1,5,6]. This parameter determines the potential of catalyst to absorb antibiotic. During zero point charge determination, 50 mL of 0.01 *M* sodium chloride was adjusted to successive initial *p*H value between 2 and 12 at 25 °C by titrating it with HCl (0.1 *M*) and NaOH (0.1 *M*), and 0.10 g catalyst was added to each solution. After 48 h, final *p*H of each solution was measured and plotted against initial *p*H. The *p*H at which curve crossed the line of equality was taken as pH_{zpc} of samples.

Results and discussion

SEM images of calcium oxide (CaO) and (Zr-TiO_2/CaO) are shown in Fig. 1(a,b). CaO surface exhibited uneven, porous surface to enhance the adsorption of Zr-TiO_2 on calcium oxide surface. These pores provided a good surface and space for possible entrapment of Zr-TiO_2 particles. Figure 1(c,d) displays the surface morphology of Zr-TiO_2/CaO at different magnification[21,22]. Zr-TiO_2/CaO is seen to be dispersed on the surface of CaO. Figure 2(a,b) depicts the TEM images of prepared Zr-TiO_2/CaO nanocomposites. Zr-doped TiO_2/CaO shows relatively non-uniform particles (50–100nm) with spherical shaped agglomerates[22]. EDX pattern of CaO indicates the presence of Ca and O element (Fig. 2c). EDX images of Zr-TiO_2 onto CaO indicates the presence of Zr and Ti on CaO surface (Fig. 2d). EDX pattern further confirms the successful attachment of Zr-TiO_2 onto CaO support.

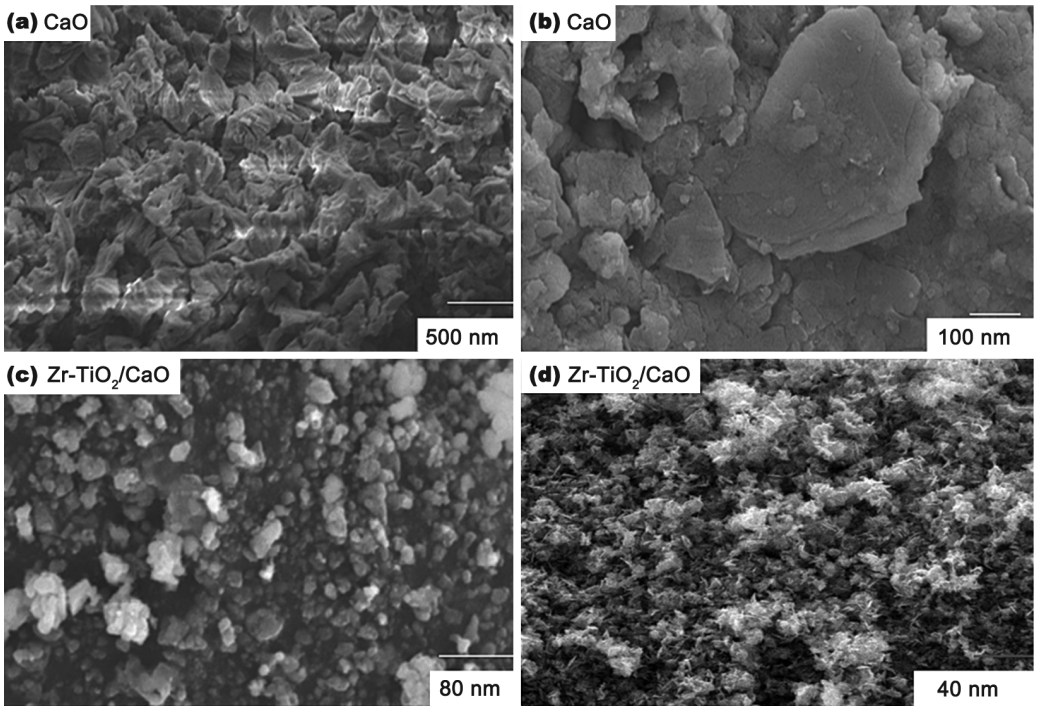

Fig. 1—SEM images of CaO (calcium oxide) (a,b) and Zr-TiO_2/CaO (c,d) at different magnifications.

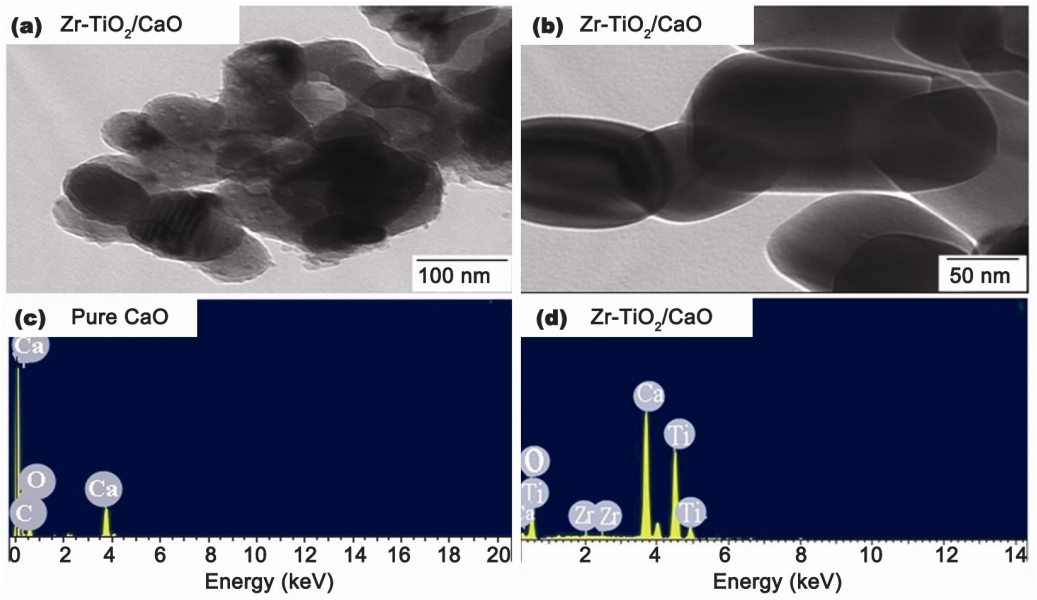

Fig. 2—(a,b) TEM pattern of Zr-TiO_2/CaO at different magnifications, (c) EDAX images of CaO, and, (d) Zr-TiO_2/CaO.

XRD pattern of Zr-TiO_2/CaO and CaO shows the prepared CaO diffraction peaks at 27.5°, 34.8°, 47.1°, 54.3°, 62.6°, 71.7° and 84.7° corresponding to (100), (111), (021), (200), (220), (041) and (311) (Fig. 3(inset). These diffraction peaks are well matched with standard (JCPDS-82-1691) for CaO[23,24]. In XRD spectra of Zr-TiO_2/CaO, the characteristics peaks of CaO was observed at 47.1°, 54.3°, 62.6° and 84.7°. The peaks at 25.0°, 38.0°, 47.9°, 55.0°, 64.3° and 70.4° correspond to planes (101), (103), (112), (000), (211) and (204) of TiO_2, respectively[22]. The additional peaks at 29.5° and 50.9° indicate the diffraction plane (111) and (220) for Zr[22]. The results are in good argument with the standard JCPDS file (JCPDS-21-1272) (and JCPDS-50-1089)[25-27].

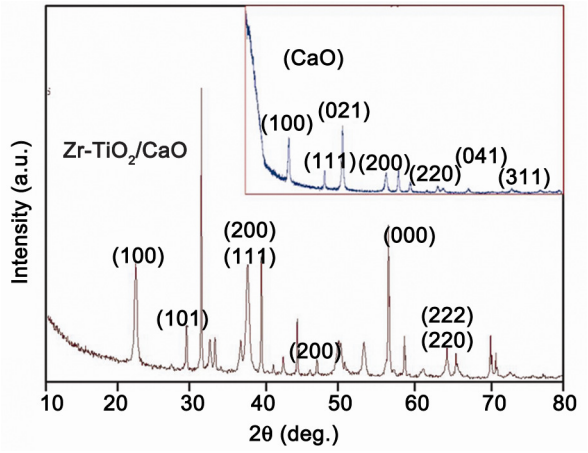

Fig. 3—XRD pattern of Zr-TiO_2/CaO. [Inset: XRD pattern of CaO].

The FTIR spectra of CaO shows the peak at 712 cm^{-1} corresponding to Ca-O bond present in CaO (Supplementary data, Fig. S1). The peaks at 1417 cm^{-1} and 866 cm^{-1} are ascribed to C-O bond present in the eggshell. The absorption peak at 3420 cm^{-1} was due to O-H bond of adsorbed water[28]. The peaks at 2923 cm^{-1} and 3399 cm^{-1} were assigned to amines and amides present in the egg shell[29]. In FTIR spectrum of Zr-TiO_2/CaO nanocomposite the band appearing at 3642 cm^{-1} corresponded to-OH stretching vibrations originating in nanocomposite[22,30]. The band at 457 cm^{-1} confirmed the presence of -O-Zr bonding. The IR peak at 448 cm^{-1} was ascribed to the stretching vibrations of -Ti-O- bonding[25]. The peaks at 566 cm^{-1} was due to the stretching vibrations of Zr-O[26]. The IR peak at 1489 cm^{-1} corresponded to stretching vibrations of C-O.

The UV-vis absorption spectrum of TiO_2 and Zr-TiO_2/CaO nanocomposite dispersed in ethanol shows he absorption maxima located at 360 nm and 380 nm, respectively (Supplementary data, Fig. S2). In comparison to TiO_2, there was a red shift towards longer wavelength in Zr-TiO_2/CaO, indicating the shift of absorption edge towards longer wavelength. The band gap of TiO_2 and Zr-TiO_2/CaO was calculated using Tauc relationship[28], $\alpha h\nu = B(h\nu - E_g)^n$, where α = absorption coefficient = 2.303 A/L, E_g= optical band gap, B = band tailing parameter, $h\nu$ is the photon energy and n = ½ for direct band gap. The band gap was determined by extrapolating straight portion of curve between $(\alpha h\nu)^2$ and $h\nu$ when $\alpha = 0$. The band gap for TiO_2 and Zr-TiO_2/CaO was found to be 3.2 and 2.95 eV, respectively. In present study, pH of zero point charge (pH_{zpc}) of Zr-TiO_2/CaO was found to be 6.2.

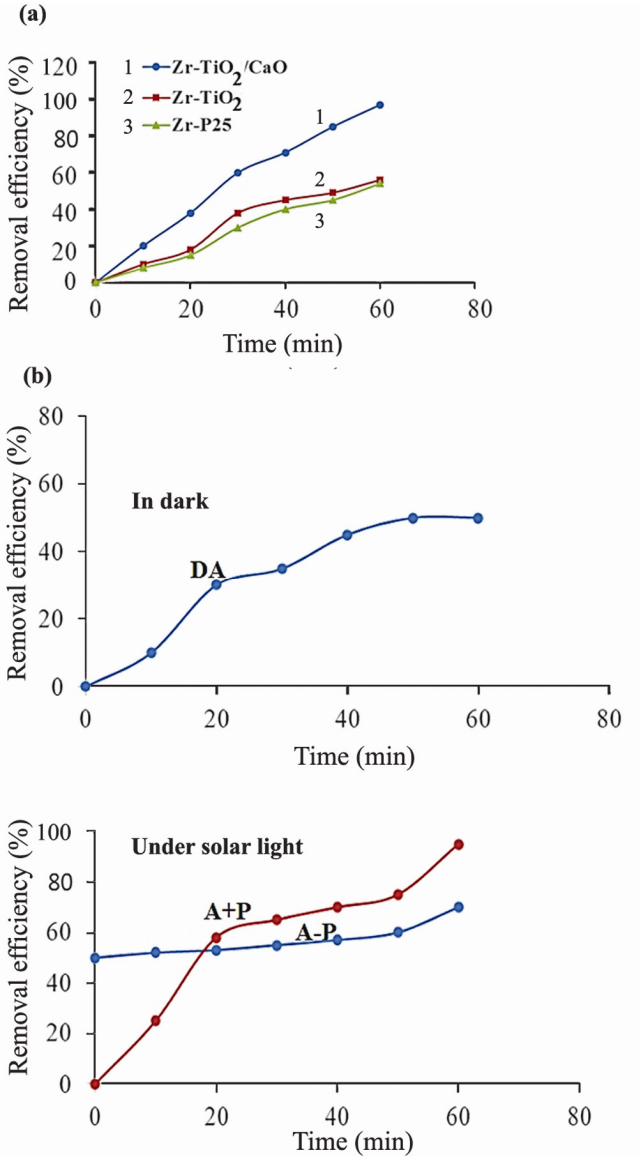

Fig. 4—(a) Degradation efficiency of different photocatalysts, and, (b) Photodegradation process using Zr-TiO_2/CaO system for OTC degradation under solar light. [React. cond.: OTC = 5×10^{-4} mol dm^{-3}, catalyst= 60 mg/50 mL, pH = 5, reaction time = 60 min, solar light intensity = 35×10^3 lx (±1000 lx).

The photocatalytic activity of Zr-TiO_2/CaO, Zr-TiO_2 and Zr-P25 was evaluated for the degradation of oxytetracycline antibiotic under solar light (Fig. 4a). The reaction system was exposed to solar light for 60 min. The efficiency of used photocatalyst followed the trend: Zr-TiO_2/CaO> Zr-TiO_2> Zr-P25. Both Zr-TiO_2/CaO and Zr-TiO_2 had higher efficiency as compared to Zr-P25. The higher photocatalytic efficiency of Zr-TiO_2 under solar light was due to extension of the absorption edge towards longer wavelength, while Zr-TiO_2/CaO was the most

efficient photocatalyst. The incorporation of CaO with Zr-TiO_2 enhanced the adsorption of antibiotics onto the catalyst surface. The adsorption of aqueous phase pollutant is regarded as an important step during the surface assisted photodegradation reactions. Further, in order to explore the role of adsorption in photodegradation processes, OTC removal was investigated under three different conditions, i.e., adsorption in dark (DA), equilibrium adsorption followed by photodegradation (A-P) and simultaneous adsorption and photocatalysis (A+P). Figure 4(b) shows the removal efficiency of Zr-TiO_2/CaO as a function of time using DA, A-P and A+P system. The first portion of graph displayed adsorption process in dark using Zr-TiO_2/CaO/DA system. While second half graph was ascribed to A-P and A+P under solar light. During simultaneous adsorption and degradation process (A+P), 97% of OTC was decolorized in 60 min. Only 53% of OTC was removed during dark adsorption. The efficiency of the investigated systems for OTC removal followed the order: Zr-TiO_2/CaO/A+P > Zr-TiO_2/CaO/A-P > Zr-TiO_2/CaO/DA. Furthermore, it was also noticed that OTC removal in A+P system was higher than in A-P system. Our results for adsorption and degradation studies are comparable with the previous work by Shon and co-worker[31]. In their studies they claimed that simultaneous activated carbon adsorption and TiO_2 photodegradation led to higher organic matter removal compared to activated carbon adsorption followed by TiO_2 photodegradation. The adsorption of adsorbate onto catalyst increased the rate of photocatalytic degradation[32]. In the present work, A-P system had lower removal efficiency in comparison to DA, due to retarding effect of adsorption on photocatalytic process. The three processes followed the efficiency: A+P > DA > A-P. The combination of Zr-TiO_2 and CaO had a synchronous effect on OTC degradation by combination of adsorption and photocatalysis, while during A+P, adsorption had retarding effect due to screening of solar light by surface adsorbed OTC molecule[33].

The effects of various reaction parameters, OTC concentration, catalyst loading and *p*H on photocatalytic activity of Zr-TiO_2/CaO A+P system were studied (Fig. 5). The results were interpreted in term of first order rate constant (k) and half-life period ($t_{1/2}$). The initial concentration of oxytetracycline was varied from 0.7×10^{-4} mol dm^{-3} to 9×10^{-4} mol dm^{-3}. The rate constant increased from 2.0×10^{-4} s^{-1} to 5.6×10^{-4} s^{-1} with the increase in the OTC concentration from

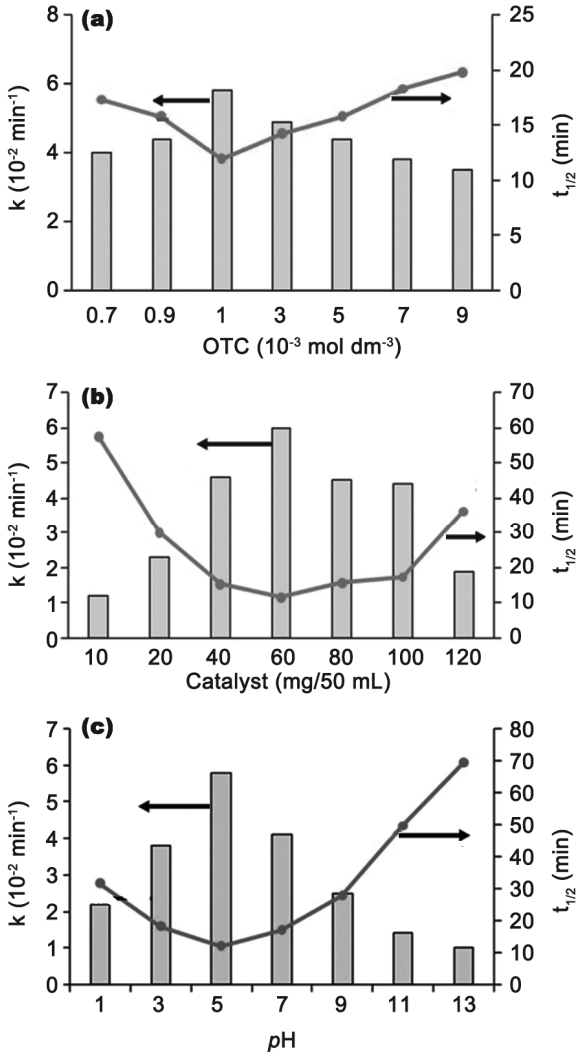

Fig. 5—Effect of reaction parameters on OTC degradation under solar Zr-TiO_2/CaOsystem. [(a) Effect of OTC concentration; (b) Effect of catalyst loading; (c) Effect of *p*H. React. cond.: OTC = 5×10^{-4}mol dm^{-3}; Zr-TiO_2/CaO = 60 mg/50 mL; *p*H = 5; reaction time = 60 min; solar light intensity = 35×10^3 lx (±1000 lx)].

0.7×10^{-4} mol dm^{-3} to 5×10^{-4} mol dm^{-3}. Thereafter, rate constant decreased from 5.6×10^{-2} min^{-1} to 3.5×10^{-2} min^{-1} with increase in oxytetracycline concentration from 5.0×10^{-4} mol dm^{-3} to 9.0×10^{-4} mol dm^{-3}. The rate constant was maximal at 5×10^{-4} mol dm^{-3} of oxytetracycline (OTC) concentration. This trend was attributed to the availability of more OTC molecules on photoactive volumes for the photodegradation process and OTC itself started acting as a filter for the incident radiation and reduced the photoactive volume. Excessive adsorption of OTC molecules onto the catalyst surface, Zr-TiO_2/CaO hindered the competitive adsorption of OH^- ions that lowered the rate of OH^- formation[35-37].

The amount of Zr-TiO_2/CaO was varied from 10 mg/50 mL to 120 mg/50 mL to explore the effect of catalyst dose for OTC degradation. Rate constant increased from 1.2×10^{-2} min^{-1} to 6.0×10^{-2} min^{-1} with increase in Zr-TiO_2/CaO loading from 10 mg/50 mL to 120 mg/50 mL. The rate constant was maximal at 60 mg/50 mL of photocatalyst loading, which can be explained in the terms of availability of active sites on Zr-TiO_2/CaO surface and penetration of visible light into the suspension. However, above the optimal concentration, excessive OTC concentration starts acting as a filter for incident light. All these factors suggest that optimal amount of Zr-TiO_2/CaO was required to avoid excess of catalyst and also to ensure availability of light photons for efficient photodegradation of OTC[22,25,38].

With the increase in *p*H from 1 to 5, the value of rate constant increased from 2.2×10^{-2} min^{-1} to 5.8×10^{-2} min^{-1} (Fig. 5c). However, the rate constant decreased with increase in *p*H from 5 to 13. The above trend can be explained on the basis of surface charge of catalyst and existence of different ionic species of OTC at different *p*H values. Above pH_{zpc}, surface of absorbents was predominantly negatively charged, while below pH_{zpc}, the positively charged species dominated the catalyst surface. The ionic species of OTC completely changed from positive charge to negative charge with change in *p*H from acidic to basic. At lower *p*H, both absorbent and antibiotic were positively charged and resulted in lower adsorption of OTC. However, majority of OTC changed to zwitterionic form[1] ($H_2OTC^{\pm}$) at *p*H 5. This resulted in higher adsorption of OTC onto the surface of Zr-TiO_2/CaO, leading to increased rate of OTC degradation. At *p*H 8.5 and 11, OTC existed mainly as $HOTC^-$ and OTC^{2-}, respectively[1,29,39]. These factors were responsible for optimal *p*H 5 of the reaction solution for photodegradation of OTC.

In order to explore the role of $OH^{\bullet}$ radical, OTC removal experiments were performed with isopropanol. Isopropanol containing α-hydrogen was highly reactive with $OH^{\bullet}$ and poorly with O_2^{-} species. Buxton and co-worker[40] reported high second order rate constant (6×10^9 M^{-1} s^{-1}) for isopropanol with $OH^{\cdot}$ radicals. The effect of isopropanol (2×10^{-4} mol dm^{-3}) on OTC degradation was investigated. The rate of OTC removal was significantly reduced in the presence of isopropanol. Only 10% of OTC was removed in the presence of isopropanol due to

$$Zr-TiO_2/CaO + h\vartheta \rightarrow Zr-TiO2/CaO\ /HA(e^-_{CB} + h^+_{VB}) \quad \ldots(5)$$

$$h^+_{VB} + OH^- \rightarrow OH\cdot \quad \ldots(6)$$

$$e^-_{CB} + O_2 \rightarrow O_2^{-}\cdot \quad \ldots(7)$$

$$H^+ + O_2^{-}\cdot \rightarrow HO_2 \quad \ldots(8)$$

$$HOTC^-(pH > 5) + h\vartheta \rightarrow HOTC^{-*} \quad \ldots(9)$$

$$HOTC^{-*} + O_2 \rightarrow HOTC\cdot + O_2^{-} \quad \ldots(10)$$

$$HOTC^- + e^-_{CB} \rightarrow OTC^{2-} \quad \ldots(11)$$

$$OTC/OTC^{2-}/HOTC\cdot + OH\cdot \rightarrow \text{degraded products} \quad \ldots(12)$$

$$OTC/OTC^{2-}/HOTC\cdot + h^+_{VB} \rightarrow \text{degraded products} \quad \ldots(13)$$

Scheme 1

quenching of $OH^{\cdot}$. These results indicate that degradation mainly occurred through $OH^{\cdot}$ radical assisted oxidative pathway.

During photocatalytic process, Zr-TiO_2/CaO produced conduction band electrons (e^-_{CB}) and valance band holes (h^+_{VB}) (Eq. 5). $OH^{\cdot}$ and ($O_2^{-\cdot}$) were also generated directly during illumination of Zr-TiO_2/CaO[41]. Photo-oxidation and adsorption occur on or near particle surface. At *p*H ≈5, $HOTC^-$ was excited to singlet state which crossed to triplet state $HOTC^{-*}$ by intersystem crossing mechanism[42]. The triplet state $HOTC^{-*}$ resulted in injection of electron in conduction band to generate superoxide anion radical ($O_2^{-\cdot}$)[41]. $HOTC^-$ also acted as electron scavenger for conduction band electrons. $HOTC^-$ also acted as a sensitizer during solar photocatalytic removal of OTC[42]. Overall mechanism can be explained by Eqs 5-13 (Scheme 1). Doping of metal atoms possibly inhibited the recombination of photo-induced electron-hole pairs[22,43].

Recycling efficiency is one of most important factor for efficient photocatalytic process. The recycling efficiency of Zr-TiO_2/CaO was explored under solar light. During each run, catalyst was separated from solution by centrifuging the photocatalyst for 2 min. The separated photocatalyst was washed and dried for further use. The efficiency of Zr-TiO_2/CaO was reduced to 74% from 90% for six consecutive cycles. However, in the case of Zr-TiO_2, the efficiency was decreased to 25% from 55%. These findings indicate that Zr-TiO_2/CaO exhibits higher recycle efficiency as compared to Zr-TiO_2.

In the present work, waste hen eggshell was used as a precursor for the preparation of CaO.

Zr doped TiO_2 was successfully synthesized by simple sol-gel method and immobilized onto CaO to prepare Zr-TiO_2/CaO. The photocatalytic activity of Zr-TiO_2/CaO was tested for the removal of oxytetracycline from aqueous phase. The prepared photocatalyst exhibited band gap of 2.95 eV. Zr-TiO_2/CaO exhibited higher photocatalytic activity as compared to Zr-TiO_2 and Zr-P25. Simultaneous adoption and photocatalysis (A+P) had synergistic effect on oxytetracycline removal. The reaction was maximal at 5×10^{-4} mol dm^{-3} of OTC concentration. The optimal catalyst loading was found to be 60 mg/50 mL, while OTC degradation was highest at *p*H 5. The degradation process mainly occurred by hydroxyl radical assisted oxidative pathway. The present study shows the applicability of Zr-TiO_2/CaO both as photocatalyst and adsorbent for wastewater remediation.

Supplementary data

Supplementary data associated with this article, i.e., Figs S1 and S2, are available in the electronic form at http://www.niscair.res.in/jinfo/ijca/IJCA_55A(07)803-809_SupplData.pdf.

References

1 Zhao C, Pelaez M, Duan X, Deng H, Shea K O & Dionysiou D D, *Appl Catal B,*134-135 (2013) 83.

2 Lanzky P F, Ingerslev F, Holten Lutzhoft H C & Jorgensen S E, *Chemosphere*, 36 (1998) 357.

3 Kümmerer K, *J Antimicrob Chemother,* 52 (2003) 5.

4 Kumar A & Xagoraraki I, *Sci Total Environ,* 408 (2010) 5972.

5 Raizada P, Singh P, Kumar A, Pathania D & Thakur P, *Appl Catal A,* 476 (2014) 9.

6 Raizada P, Singh P, Kumar A, Pare B & Jonnalgadda S B, *Sep & Purif Technol*, 133 (2014) 429

7 Hoffmann M R, Martin S T, Choi W Y & Bahnemann D W, *Chem Rev*, 95 (1995) 69.

8 Kim S, Hwang S J & Choi W, *J Phys Chem* B, 109 (2005) 24260.

9 Chen D, Yang D, Wang Q & Jiang Z Y, *Ind Eng Chem Res*, 45 (2006) 4110.

10 Bakshi M S, Thakur P & Banipal T S, *Mater Lett*, 61 (2007) 3762.

11 Toyoda T, Kawano H, Shen Q, Kotera A & Ohmori M, *J Appl Phys Part 1*, 39 (2000) 3160.

12 Asahi R, Morikawa T, Aoki K & Taga Y, *Science*, 293 (2001) 269.

13 Cheng P, Zheng M, Y Jin, Huang Q & Gu M, *Mater Lett*, 5(2003) 2989.

14 Geng H, Yin S, Yang X & Liu B, *J Phy Condens Mater*, 18 (2006) 87.

15 Parra D R, Pulgarin S, Hrzton A C & Weber V, *Appl Surf Sci*, 167 (2000) 51.

16 Qourzal S, Tamimi M, Assabbane A & Aitichou Y, *J Colloid Interf Sci*, 286 (2005) 621.

17 Singh P, Raizada P & Pathania D, *Indian J Chem Technol,* 20 (2013) 305.

18 Olga B K, Isabelle L & Alexander V, *Chem Mater*, 9 (1997) 2468.

19 Tangboriboon N, Kunanuruksapong R & Sirivat A, *Mater Sci-Poland*, 30 (2012) 313.

20 Supphasrirongjaroen P, Praserthdam P & Panpranot, *J Ceram Int*, 36 (2010) 1439.

21 Kim C S, Shin J W, Jang H D & Kim T O, *Chem Eng J*, 204 (2012) 40.

22 Kambur A, Pozan G S & Boz I, *Appl Catal B, Environ*, 115 (2012) 149.

23 Balazsi C, Kover Z, Horvath E & Weber F, *Mater Sci Forum*, 537 (2007) 105.

24 Liu S, Maa J, Li J & Sun Y, *Micro Meso Mater*, 117 (2009) 466.

25 Mu J, Bui D N, Kang S Z & Li X, *Catal Commun*, 13 (2011) 14.

26 Vijaya J J, Selvam N C S, Manikandan A & Kennedy L J, *J Colloid Interf Sci*, 389 (2013) 91.

27 Pantelides S T, *Rev Mod Phys*, 50 (1978) 797.

28 Roy A & Bhattacharya J, *Int J Nanosci*, 10 (2011) 413.

29 Tsai W T, Yang J M, Lai C W, Lin C C & Yeh C W, *Biores Technol,* 97 (2006) 488.

30 Wu L, Yu J C, Zhang L, Wang X & Ho W, *J Solid State Chem*,17 (2004) 2584.

31 Shoun H K, Vigneswaran S, Ngo H H & Him J H, *Water Res*, 39 (2005) 2549.

32 Jo WK, Shin S H & Hwang E S, *J Hazard Mater*, 191 (2011) 234.

33 Xiong L, Sun W, Yang Y, Chen C & Ni J, *J Colloid Interf Sci*, 356 (2011) 211.

34 Pare B, Singh P & Jonnalagadda S B, *Indian J Chem Technol*, 17 (2010) 391.

35 Nakano, TIkawa N I & Ozimek L, *Poultry Sci,* 82 (2003) 510.

36 Raizada P & Sharma U, *Indian J Chem Technol*, 17 (2010) 267.

37 Raizada P, Singh P, Kumar A, Pathania D & Thakur P, *Appl Catal A*, 486 (2014) 159.

38 Gao B, Lim T M, Subagio D P & Lim T T, *Appl Catal A*, 375 (2010) 107.

39 Elmolla E S & Chaudhuri M, *J Hazard Mater*, 173 (2010) 445.

40 Buxton V, Greenstock C, Hellman W P & Ross A B, *J Phys Chem Ref Data,* 17 (1988) 513.

41 Singh P, Raizada P, Kumar A & Thakur P, *Int J Photoenergy,* 7 (2013) 7.

42 Zhao C, Pelaez M, Duan X & Dionysiou D D, *Appl Catal B,* 134 (2013) 83.

43 Umebayashi T, Yamaki T & Asai K, *J Phys Chem Solids*, 63 (2003) 1909.